HHS Public Access

Author manuscript

Alzheimers Dement. Author manuscript; available in PMC 2024 January 01.

Published in final edited form as:

Alzheimers Dement. 2023 January ; 19(1): 169–180. doi:10.1002/alz.12656.

Waning locus coeruleus integrity precedes cortical tau accrual in preclinical autosomal dominant Alzheimer's disease

Heidi I.L. Jacobs, Ph.D.[a,b], **John Alex Becker, Ph.D.**[a], **Kenneth Kwong, Ph.D.**[c], **Diana Munera, BS**[d], **Liliana Ramirez-Gomez, M.D.**[e], **Nina Engels-Domínguez, MSc.**[a,b], **Justin S. Sanchez, BA**[a], **Clara Vila-Castelar, Ph.D.**[d], **Ana Baena, MA**[f], **Reisa A. Sperling, M.D.**[c,e,g], **Keith A. Johnson, M.D.**[a,g], **Francisco Lopera, M.D.**[f], **Yakeel T. Quiroz, Ph.D.**[d,e,f,*]

[a]Gordon Center for Medical Imaging, Department of Radiology, Massachusetts General Hospital/ Harvard Medical School, Boston, MA, USA

[b]Faculty of Health, Medicine and Life Sciences, School for Mental Health and Neuroscience, Alzheimer Centre Limburg, Maastricht University, Maastricht, The Netherlands

[c]Athinoula A. Martinos Center for Biomedial Imaging, Department of Radiology, Massachusetts General Hospital/Harvard Medical School, Boston, MA, USA

[d]Department of Psychiatry, Massachusetts General Hospital/Harvard Medical School, Boston, MA, USA

[e]Department of Neurology, Massachusetts General Hospital/Harvard Medical School, Boston, MA, USA

[f]Grupo Neurociencias de Antioquia, Universidad de Antioquia, Medellín, Colombia

[g]Center for Alzheimer Research and Treatment, Department of Neurology, Brigham and Women's Hospital, Harvard Medical School, Boston, M, USA

Abstract

INTRODUCTION: Autopsy studies recognize the locus coeruleus (LC) as one of the first sites accumulating tau in Alzheimer's disease (AD). Recent AD work related in-vivo LC MRI-integrity to tau and cognitive decline; however, relationships of LC integrity to age, tau and cognition in autosomal dominant AD (ADAD) remain unexplored.

METHODS: We associated LC integrity (3T-MRI) with estimated-years-of-onset, cortical beta-amyloid, regional tau (PET) and memory (CERAD Word-List-Learning) among 27 carriers and 27 noncarriers of the *PSEN1 E280A* mutation. Longitudinal changes between LC integrity and tau were evaluated in 10 carriers.

RESULTS: LC integrity started to decline at age 32 in carriers, 12 years before clinical onset, and 20 years earlier than in sporadic AD. LC integrity was negatively associated with cortical tau, independent of beta-amyloid, and predicted precuneus tau increases. LC integrity was positively associated with memory.

[*]Corresponding author: Yakeel T. Quiroz, PhD; Departments of Psychiatry and Neurology, Massachusetts General Hospital, 100 1st Avenue, Building 39, Suite 101, Charlestown, MA 02129, Phone: (617) 643-5944; Fax: (617) 726-5760; yquiroz@mgh.harvard.edu.

DISCUSSION: These findings support LC integrity as marker of disease progression in preclinical ADAD.

Keywords

Alzheimer's disease; tau; locus coeruleus; brainstem; autosomal dominant; early onset

1. Background

Alzheimer's disease (AD), the most common form of dementia, is neuropathologically defined by accumulation of beta-amyloid (Aβ) plaques and neurofibrillary tangles [1, 2]. Each of these pathologies follow a distinct, but predictable topography in the brain [3]. At the age of 40, nearly every autopsy case exhibits hyperphosphorylated tau in the locus coeruleus (LC) [2, 4, 5]. Then, around age 50 tau emerges in the entorhinal cortex, followed in a subset by accumulation of Aβ and tau in the neocortex starting around age 60 [2, 3]. The clinical symptoms in sporadic AD are typically observed beginning after age 65. These time lags between pathology and clinical symptoms may be crucial to determine when interventions should be initiated. Earlier detection and intervention are critical to prevent rampant spreading of pathology and delay disease progression. The LC is an important target, given its early vulnerability to tau aggregation and important role in the modulation of cognition [6].

Among older individuals, including preclinical sporadic AD, we recently demonstrated with dedicated MRI-methods that LC intensity$_r$ (relative intensity to pontine tegmentum, likely reflecting integrity[7]) peaks and starts to decline at age 54, a time in life when cortical tau starts to set in [7]. Consistent with autopsy data, lower LC intensity$_r$ was associated with greater allocortical tau binding, also in individuals in whom Aβ was not yet detectable. Lower LC intensity$_r$ also predicted memory decline, prior to the presence of readily detectable levels of fibrillar Aβ-PET levels [7]. These findings are significant as they indicate that LC MRI-measures can be a promising indicator of initial AD-related processes [8].

Individuals carrying Presenilin-1 (*PSEN1*) mutations are preordained to develop autosomal dominant Alzheimer's disease (ADAD) early in adulthood [9]. While the pathologies in sporadic AD and ADAD are similar, they differ in temporal ordering. In ADAD, Aβ deposition precedes cortical tau pathology by approximately 10–15 years [9–11]. Cortical tau pathology in ADAD is known to occur nine years prior to disease onset, topographically similar to sporadic AD, but with an accelerated progression. Autopsy studies have not yet systematically examined the LC in ADAD, but the LC of a younger case with Braak stage VI (#63) in Theofilas et al. (2017) encompassed one third of the neurons relative to the other older Braak VI cases, indicating a more aggressively affected LC in early-onset AD [12]. In addition, alterations in norepinephrine transmission and metabolism are evident in sporadic and early-onset AD [13, 14], and linked to tau and cognitive decline [15, 16]. Given that the LC is an initial site of pretangle material in AD, and that tau is closely associated with cognition, we hypothesized that in ADAD age-related changes in LC intensity$_r$ occur early in adulthood, before accumulation of tangle pathology but likely shortly after the expected

onset of Aβ. In addition, we expected that worse LC intensity$_r$ would be associated with greater cortical tau deposition, and worse cognitive performance.

To examine these hypotheses, we related LC intensity$_r$ using MRI, to Aβ and tau using PET and cognitive measures in *PSEN1 E280A* (Glu280Ala) mutation carriers from the largest known kindred, residing in Antioquia, Colombia, and age-matched noncarrier family members. A subset of these carriers also had follow-up imaging and cognitive data after on average two years, allowing us to assess whether LC intensity$_r$ tracks with tau changes, and determining whether LC intensity$_r$ may hold promise in the search for an early prognostic marker.

2. Methods

2.1. Participants

Twenty-seven mutation carriers (19 cognitively unimpaired and eight impaired; age range:28.5–49.25), and 27 noncarriers (age range:28.5–47.25) from the Massachusetts General Hospital (MGH) COLBOS (Colombia-Boston) Biomarker study were included. Participants were recruited from the Colombian Alzheimer's Prevention registry. Exclusion criteria included: diagnosis of dementia, a medical, psychiatric or neurological disorder, a history of stroke, seizures, substance abuse or other disorders affecting motor, visuospatial or cognitive abilities. Individuals were considered cognitively unimpaired if they exhibited no impairment on the Consortium to Establish a Registry for Alzheimer's Disease neuropsychological battery (CERAD) word list recall and visuospatial memory tests, scored at least 26 or more on the Mini-Mental State Examination (MMSE), received a score of 0 on the clinical dementia rating (CDR) scale and scored below 3 on the Functional Assessment Staging Test (FAST). Impaired carriers were those who met criteria for mild cognitive impairment, had a CDR of 0.5 and a FAST > 3. The expected years to onset (EYO) was calculated by subtracting the carriers' age from 44, median age of clinical onset in *PSEN1* E280A carriers (95%CI = 43–45)[17] and only used in the interpretation of the estimated sequence of biomarker changes. For ten carriers, we also obtained follow-up imaging data (median follow-up time: 2 years, IQR[1.81, 3.5] [18].

Participants traveled from Colombia to Boston to undergo MRI and PET imaging at MGH, and neuropsychological assessments were conducted in Spanish at the University of Antioquia within 6 months of imaging. All participants provided informed written consent and protocols were approved by the local institutional review boards of the University of Antioquia and MGH. Investigators and participants were blinded to carrier status.

2.2. Magnetic resonance imaging

Magnetic resonance imaging was performed at MGH on a 3T-imaging system (TIM Trio; Siemens). Structural 3D T1-weighted magnetization–prepared rapid-acquisition gradient-echo (MPRAGE) images were collected (repetition time=2300ms, echo time=2.95ms, flip angle=9°, 1.05×1.05×1.20mm resolution). To visualize the LC, we applied a 2D-T1-weighted Turbo-Spin-Echo (TSE) sequence with MT contrast (repetition time=743ms,

echo time=16ms, flip angle=180°, 6 slices, 4 online averages, 0.4×0.4×3.00mm resolution, acquisition time:3:24min).

T1-weighted images were processed using FreeSurfer (FS) version 6.0.0 using the default automated reconstruction protocol [19]. To calculate signal intensity$_r$ in the LC, we applied the method reported previously [7]. In summary, search-regions in MNI-space covering the bilateral LC region and rostral pontine tegmentum (reference) were warped to each individual LC-scan using the high-dimensional symmetric diffeomorphic normalization transformation of the Advanced Normalization Tool (ANTs, Philadelphia, USA)[20], and visually checked. We normalized each slice to the average intensity of the reference region to remove interslice variability and potential age-confounding effects from the reference region. Consistent with others as well as our previous work [7, 21–23] reporting a good signal-to-noise distribution, we applied an iterative search-algorithm within these search-regions to obtain the highest intensity value in 5 connecting voxels. Autopsy work did not report asymmetry in LC tau or neuronal changes [24] and consistent with our previous work [7], we averaged the left and right extracted intensities.

2.3. Positron emission tomography

The Pittsburgh Compound B (PiB)-PET and Flortaucipir (FTP)-PET data were acquired at MGH on a Siemens/CTI ECAT HR+ scanner [25, 26]: PiB-PET was acquired with bolus injection (8.5–15 mCi) followed immediately by a 60-minute dynamic acquisition in 69 frames (12×15 seconds, 57×60 seconds) and FTP was acquired from 75–105 minutes after bolus injection (9.0–11.0 mCi) in 4×5-minute frames. PET data were reconstructed applying standard data corrections [25].

To evaluate the anatomy of cortical FTP binding, each individual PET-data set was rigidly coregistered to the subject's MPRAGE data. The FS's region-of-interest (ROIs) were transformed into PET native space. PiB-PET data were expressed as the distribution volume ratio (DVR) with cerebellar grey as reference using the Logan graphical method applied to data from the 40–60-minute post-injection integration interval. PiB-status was ascertained in a neocortical aggregate region using a 1.20 DVR cut-off based on Gaussian Mixture Modeling in an independent dataset [27]. Given the high correlation across many cortical regions and to avoid noise introduction PiB-data did not undergo partial volume correction (PVC). Regional FTP-PET data were PVC using the Geometrical Transfer Matrix method[28], assuming a uniform 6mm point spread function. For surface-based FTP-PET analyses, we implemented the extended Muller-Gartner correction for PVC in volume space prior to surface sampling, and then applied surface-smoothing equivalent to 8mm FWHM Gaussian kernel. Regional FTP binding was expressed in FS-defined regions reflecting critical Braak-stages (entorhinal (stage I-II), inferior temporal (stage IV) and precuneus (stage V)) as standardized uptake value ratio (SUVr) using cerebellar grey as reference.

2.4. Statistical analyses

Statistical analyses were performed using the R-software (version 3.5.1). Given the non-Gaussian distribution of our biomarker and cognitive variables, group differences were

tested using the Wilcoxon-rank test for continuous variables, the Kruskal-Wallis test when comparing more than two groups, and the Fisher-exact test for dichotomous variables.

Age-relationships with LC intensity$_r$ (including quadratic terms) were tested using linear regression analyses with bootstrapping of the standard error of the estimates over 5,000 replicates. To determine the peak of the quadratic age-function, we calculated the first derivative and its 95% confidence interval using central finite differences. To understand the age-positioning of the LC data in (preclinical) ADAD relative to individuals with preclinical AD, we matched LC intensity$_r$ of the (unimpaired) carriers to participants of the Harvard Aging Brain Study (n=155, ages 50–94 years, 27.75% PiB+)[7]. Matching was done using non-parametric greedy nearest neighbor matching on a propensity score using a logistic regression of the carriers on PiB DVR and entorhinal FTP SUVr. Balance was assessed with mean standardized differences for both variables, and if needed also their interaction, before and after matching. Relationships between age and LC intensity$_r$ between carriers and matched older participants were compared using bootstrapped linear regression.

Associations between LC intensity$_r$ and tau or Aβ-PET measures or cognitive performance were examined using bootstrapped linear regression analyses. Given that age is synonymous with disease stage in this population, we took a hierarchical approach for the PET-analyses: 1) without covariates, 2) including age and sex as covariate, and 3) excluding impaired carriers. In addition, for FTP-PET analyses, we also ran analyses with PiB-PET as covariate. For cognition, we z-transformed CERAD word list scores using age-adjusted residuals of noncarriers and included sex and education as covariates in the regression. PET-associations were confirmed with vertex-wise partial Spearman-rank correlations between LC intensity$_r$ and tau or Aβ within all carriers or within unimpaired carriers (regressing age out). To mitigate inflated type 1 errors and take the point-spread function of PET data on surface areas into account, we applied a cluster-wise threshold of $p<0.01$ (and $p<0.05$ for the smaller longitudinal dataset) with a minimal surface-area size of 120mm^2.

Mediation analyses were performed using the quasi-Bayesian Monte Carlo approximation (1,000 simulations per vertex for surface-based and 10,000 simulations for ROI-analyses) in which the posterior distribution of quantities of interest is approximated by their sampling distribution. Proportion mediated is expressed as the mediated effect divided by the total effect.

Finally, for longitudinal analyses in the carriers, we performed linear mixed effects models (random intercept for each subject) for baseline versus change (effect size of variable of interest is expresses as partial R^2 (R^2_p)), and for change on change analyses we performed repeated measures correlation, bootstrapped over 1,000 replicates. Repeated measures correlation has the advantage that it does not require a large sample size for paired-repeated measures by taking the intra-individual variance into account (similar to random intercept) [29]. The threshold for statistical significance was set at $p<0.05$. We reported the overall model significance, reported p-values are two-sided, and 95% confidence intervals are bootstrapped.

3. Results

3.1. Age-relationship with LC intensity$_r$

Carriers and noncarriers did not differ in age, education or proportion of females (Table 1). Impaired carriers (n=8) were older than unimpaired carriers or noncarriers ($p<0.001$). All carriers exhibited lower MMSE-scores and higher PiB compared to noncarriers. LC intensity$_r$ values were similar across both groups, but impaired carriers showed lower LC intensity$_r$ compared to unimpaired carriers and noncarriers ($p=0.038$, Figure 1A). There were no sex differences in LC intensity$_r$ across the entire group ($p=0.085$) or in interaction with carrier-group ($p=0.22$).

We observed a nonlinear age-relationship with LC intensity$_r$ across the entire group (Model $p=0.04$; $\beta=-0.10$, $t(51)=-2.11$, $p=0.040$, 95%CI[−0.20,−0.01], Figure 1B). When examining this age-relationship separately for carriers and noncarriers, we observed a positive age-relationship in noncarriers ($r=0.44$, $p=0.02$) and a negative age-relationship in carriers ($r=-0.67$, $p<0.001$, Fisher $z=-4.48$, $p<0.001$) with a peak at 31.5 years (95%CI[30.3,32.7]; EYO= −12.5 95%CI[−13.7,−11.3], Figure 1C). These effects remained the same when excluding the impaired carriers (Figure S2-A).

To understand the trajectory of age-relationships with LC intensity$_r$ in ADAD relative to individuals on a trajectory to sporadic AD (n=155, Table S1), we identified a matched independent group using propensity-based matching and compared these to the carriers. Optimal matching was only possible for a model including PiB DVR, entorhinal FTP SUVr and their interaction (Figure 1D; Figure S1 for love plots of all matching results). There was no difference between carriers and the matched group in terms of PiB DVR ($p=0.85$), entorhinal FTP SUVr ($p=0.62$) or LC intensity$_r$ ($p=0.89$). The age-range of the matched group was 57–92 years (median:77.5 years, IQR [68.00,82.88]). LC intensity$_r$ was linearly related with age in the matched group ($r=-0.49$, $p=0.012$), though less steep than the carriers (Model $p<0.001$; $\beta=0.003$, $t(49)=2.29$, $p=0.026$, 95%CI[0.001,0.006], Figure 1E). These patterns were similar when matching only unimpaired carriers (Figure S2-B).

3.2. Lower LC intensity$_r$ is associated with cortical tau in carriers

Lower LC intensity$_r$ was more strongly associated with greater entorhinal FTP binding in carriers than noncarriers (Model $p<0.001$; $\beta=6.43$, $t(50)=2.72$, $p=0.009$, 95%CI[1.85,11.85]), even when excluding the impaired carriers (Model $p<0.001$; $\beta=5.39$, $t(42)=3.49$, $p=0.001$, 95%CI[2.37,8.41]), or when controlling for PiB (Table S2). The relation between LC intensity$_r$ and entorhinal FTP was trend-level when covarying for age and sex (Model $p<0.001$; $\beta=3.51$, $t(48)=1.90$, $p=0.065$, 95%CI[−0.11,7.12]). We also observed stronger negative associations between LC intensity$_r$ and FTP in inferior temporal cortex and precuneus in carriers compared to noncarriers (models $p<0.001$; IT:$\beta=6.37$, $t(50)=2.92$, $p=0.005$, 95%CI[3.40,12.47]; PRC:$\beta=12.05$, $t(50)=2.86$, $p=0.006$, 95%CI[6.60,25.51], Figure 2A), also when adjusting for age and sex (models $p<0.001$; IT:$\beta=2.56$, $t(48)=2.26$, $p=0.029$, 95%CI[0.34,4.79];PRC:$\beta=5.81$, $t(48)=2.67$, $p=0.01$, 95%CI[1.56,10.07]) or excluding impaired carriers (models $p<0.001$; IT:$\beta=3.98$, $t(42)=4.12$, $p<0.001$, 95%CI[2.06,7.37];PRC:$\beta=6.72$, $t(42)=4.26$, $p<0.001$, 95%CI[2.95,9.80]). These

group differences were independent of PiB however, when excluding impaired carriers and controlling for PiB, PiB no longer contributed and the interaction between group and LC intensity$_r$ on tau remained significant (Table S2).

Our vertex-wise correlations between LC intensity$_r$ and cortical FTP binding in carriers indeed supported widespread negative correlations in medial and lateral temporoparietal regions (Figure 2B, Table S3). The magnitude of these correlations was lower but remained significant with an overlapping spatial layout in the unimpaired carriers (Figure 2C). The vertex-wise map of noncarriers did not survive cluster-wise correction (not shown).

3.3. Lower LC intensity$_r$ is associated with neocortical Aβ deposition

Lower LC intensity$_r$ was more strongly associated with greater neocortical PiB binding in carriers than noncarriers (model $p<0.001$; $\beta=2.15$, $t(49)=3.06$, $p=0.004$, 95%CI[0.468,3.642], Figure 3A). This difference remained significant when adjusting for age and sex (model $p<0.001$; $\beta=1.55$, $t(47)=2.33$, $p=0.03$, 95%CI[0.25,2.86]), and was at-trend level when excluding impaired carriers (model $p<0.001$; $\beta=1.42$, $t(41)=2.07$, $p=0.05$, 95%CI[−0.608,3.803]). Vertex-wise correlations between LC intensity$_r$ and cortical PiB confirmed widespread negative correlations in medial and lateral frontal regions in carriers (Figure 3B, Table S3). The vertex-wise map in noncarriers did not survive cluster-wise correction (not shown).

3.4. Neocortical tau mediates the relationship between LC intensity$_r$ and memory in carriers

Lower LC intensity$_r$ was associated with worse delayed recall in carriers relative to noncarriers (interaction LC intensity$_r$ by group: model $p<0.001$; $\beta=-18.64$, $t(47)=-2.24$, $p=0.030$, 95%CI[−36.39,−1.01], but this difference was driven by impaired carriers (excluding impaired carriers: $\beta=-4.11$, $t(40)=-0.53$, $p=0.60$). The groups did not differ on the association between LC intensity$_r$ and total learning (model $p<0.001$; $\beta=-6.38$, $t(47)=-0.95$, $p=0.35$, 95%CI[−20.43,6.02], Figure 4A). Vertex-wise mediation analyses revealed that tau in temporoparietal regions, including bilateral precuneus, mediates the relationship between LC intensity$_r$ and delayed recall in all carriers (Figure 4B, Table S4). ROI-based mediation analyses using precuneus FTP confirmed this: mediation effect:$\beta=17.38$,95%CI[7.45,29.97],$p=0.006$, proportion mediated:$\beta=0.72$, 95%CI[0.40,1.62],$p=0.008$ (Figure 4C).

3.5. LC intensity$_r$ and longitudinal changes in tau

Ten carriers had follow-up measurements. Lower baseline LC intensity$_r$ was associated with increases in precuneus FTP, but not with entorhinal or inferior temporal FTP changes (EC:$\beta=0.04$, $t(8)=0.04$, $p=0.97$, $R^2_p=0.00$; IT:$\beta=-2.15$, $t(8)=-1.38$, $p=0.20$, $R^2_p=0.12$; PRC:$\beta=-5.27$, $t(8)=-2.85$, $p=0.022$, $R^2_p=0.18$, 95%CI[−8.95,−1.76]; Figure S2). Associations with precuneus FTP survived correction for baseline PiB ($\beta=-5.38$, $t(7)=-2.78$, $p=0.027$, $R^2_p=0.12$, 95%CI[−9.97,−0.80]). LC intensity$_r$ declined significantly over time ($\beta=-0.011$, $t(8)=-3.00$, $p=0.015$, $R^2_p=0.47$, 95%CI[−0.012,−0.002]), independent of age ($\beta=-0.005$, $t(8)=-3.29$, $p=0.011$, $R^2_p=0.57$, 95%CI[−0.009,−0.002], Figure S4). Decreases in LC intensity$_r$ were associated with increases in FTP only in the precuneus (EC:$r_{rm}=-0.26$,

95%CI[−0.93,0.85], p=0.44; IT:r_{rm}=−0.31, 95%CI[−0.81,0.52], p=0.35; PRC:r_{rm}=−0.62, 95%CI[−0.91,−0.46], p=0.042, Figure 5A–B), which did not survive adjustment for baseline PiB (r_{rm}=−0.33, p=0.21). These associations were not driven by impaired carriers, as decreases in LC intensity$_r$ were associated with increases in entorhinal and precuneus FTP in unimpaired carriers (n=7; EC:r_{rm}=−0.84, 95%CI[−0.98,−0.08], p=0.009; IT:r_{rm}=−0.55, 95%CI[−0.94,0.47], p=0.16; PRC:r_{rm}=−0.77, 95%CI[−0.97,−0.11], p=0.025, Figure 5A–C, Table S5). In unimpaired carriers, only the change-on-change association for precuneus FTP survived adjustment for PiB (r_{rm}=−0.84, 95%CI[−0.99,−0.13],p=0.001).

4. Discussion

Autopsy studies and our previous neuropathology - neuroimaging work revealed the LC as one of the first regions affected by tau in AD, possibly decades before cortical tau accumulation and emergence of cognitive deficits [2, 4, 5, 30], and that MRI-derived LC intensity$_r$ tracks with these initial AD-related processes [7]. Here we sought to examine whether LC intensity$_r$ also correlated with cross-sectional observations and longitudinal changes in cortical tau and memory in ADAD, and to obtain more insight into the temporal emergence of LC changes within the pathophysiologic sequence of ADAD. In ADAD, age is commonly used as a proxy of disease progression, because as carriers age, they get closer to their age of estimated symptom onset. Therefore, we examined the relationship between age and LC intensity$_r$ and determined that changes in LC intensity$_r$ occur approximately 12 years prior to clinical onset, which according to disease models is after fibrillar Aβ is detectable (~16 EYO) [31, 32], but before cortical tau is evident with PET-imaging [9–11]. Even though the pathophysiologic cascade of ADAD differs from sporadic late-onset AD, they are related, and based on the estimated sequence of biomarker changes (using the EYO), our data suggests that the LC undergoes changes before accrual of cortical tau. The non-linear age-relationship with LC intensity$_r$ is consistent with other LC-imaging studies in aging or sporadic AD [7, 33, 34]. However, in ADAD the peak in LC intensity$_r$ occurs at least twenty years earlier than in sporadic AD and the negative slope between age and LC intensity$_r$ is steeper in our (preclinical) ADAD sample as compared to our previous work in preclinical sporadic AD. This indicates that even in the preclinical stages ADAD is characterized by a more accelerated disease progression [35–37]. The positive age-relationship with LC intensity$_r$ in young noncarriers is consistent with previous imaging and immunohistochemistry reports [34, 38], and has been associated with greater cognitive reserve and performance [22, 39].

Cross-sectionally, LC intensity$_r$ was associated with tau deposition in the entorhinal cortex, inferior temporal cortex and precuneus in ADAD carriers. These associations occurred independently of Aβ. Similarly, in the longitudinal analyses, a waning LC intensity$_r$ signal was associated with rises in precuneus tau in unimpaired carriers, even when taking Aβ into account. These findings indicate that in the preclinical stages of ADAD LC intensity holds promise to predict propagation of tau into the neocortex.

These longitudinal associations between LC intensity$_r$ and tau were only observed for the precuneus, which reflects a spatial pattern that is consistent with previous reports and the temporal cascade of ADAD [9, 10]. Medial temporal tauopathy is estimated to be detectable

as early as 9 EYO, 3 years prior to neocortical tau, which occurs closer to clinical onset in ADAD [11]. Medial temporal lobe tau may reach a plateau when tau is expanding and rising in other cortical regions [40, 41]. This plateauing of tau, and the temporal proximity of LC intensity$_r$ to Aβ and medial temporal tau may explain overlapping proportions of variance of these markers. Even though entorhinal tau is less dynamic and serial LC data may presage expansion of tau in the neocortex, cross-sectionally, LC intensity$_r$ measures may have an equally and potentially larger effect on initial entorhinal tau relative to Aβ in preclinical AD [42]. This is supported by recent work on CSF p-tau reporting that these non-fibrillar tau markers become elevated contemporaneously with amyloidosis, 15–20 EYO in ADAD [43, 44]. Animal studies also provided evidence linking early pathologic changes in the LC to cortical fibrillar proteinopathies. Both Aβ-oligomers binding to alpha-adrenergic receptors in LC neurons [45] as well as aberrant norepinephrine metabolism [46] are able to set off a tau hyperphosphorylation signaling cascade. We previously demonstrated that LC intensity$_r$ measures may capture processes related to these early abnormal tau changes, and the findings here extend this to also imply a prognostic role for LC intensity$_r$. In contrast to sporadic late-onset AD, we did not see consistent associations between LC intensity$_r$ and inferior temporal tau. This corroborates previous reports of a different topography of tau spreading, in which Braak stage IV is skipped in ADAD [9, 11].

Consistent with AD and ADAD disease models [47, 48] and observations in AD [7, 49], lower LC intensity$_r$ was associated with lower delayed recall performance in carriers, which was partially mediated by tau deposition in temporoparietal regions. The association with predominantly retrieval processes is congruent with our observations in sporadic AD [7] and norepinephrine's role in synaptic plasticity and long-term potentiation, the cellular process underlying learning and creating stronger memories [50]. Effect sizes for associations between LC intensity$_r$ and memory were smaller than those observed for pathology. Our sample was predominantly unimpaired and therefore, longer follow-up may be required to detect clinically meaningful sequala.

Our study has limitations. First, our cross-sectional sample size is modest, and small for repeated measures due to the international logistics of the study, bringing participants from Colombia to Boston. But, importantly, this is a homogenous sample consisting of a single *PSEN1* mutation. In addition, our findings were consistent with observations in sporadic AD and the moderate to large effect sizes support the robustness of these findings. Second, cautiousness is required when interpreting the temporal sequence across biomarkers, as the detection ability of each biomarker is limited, particularly for measuring non-fibrillar pathology. Therefore, validating our findings in postmortem and larger longitudinal studies with multiple timepoints to allow for accurate change-on-change modeling will be paramount.

In sum, LC intensity$_r$ changes early in the course of ADAD, possibly before detection of initial cortical tangle deposition, and is associated with the early pathologic and clinical phenotypes of ADAD. Though further research should confirm the directionality and mechanism of tau spreading, our findings indicate that LC intensity$_r$ decreases can predict expansion of tau into the neocortex, emphasizing the potential of LC intensity$_r$ as marker of disease progression, in particular in the preclinical phase of ADAD.

Supplementary Material

Refer to Web version on PubMed Central for supplementary material.

Acknowledgments

The authors thank the *PSEN1* Colombian families for contributing their valuable time and effort, without which this study would not have been possible. We thank the research staff of the Group of Neuroscience of Antioquia for their help coordinating study visits for the COLBOS project.

Funding sources

Dr. Quiroz was supported by grants from the NIH Office of the Director (DP5OD019833), National Institute on Aging (R01AG054671), the Alzheimer's Association, and Massachusetts General Hospital ECOR. Dr. Lopera was supported by NIA, API Colombia, and an Anonymous Foundation. Dr. Jacobs receives funding from the NIH-NIA R01AG062559, R01AG068062 and R21AG074220. Dr. Sperling receives research support for NIH grants P01AG036694, P50AG005134, 2009–2020, and U19AG10483, as well as from Eli Lilly (clinical trial) and the Alzheimer's Association. Dr. Johnson has received support from a joint NIH-Lilly-sponsored clinical trial (A4 Study - U19AG10483) and received research support from NIH grants R01AG027435, P50AG00513421, P01AG036694, R01AG046396, and U01AG024904, as well as the Alzheimer Association and Marr Foundation. Dr. Vila-Castelar receives funding from the Alzheimer's Association (2019-AARF-644631).

Conflicts of interest

KAJ has served as paid consultant for Janssen, Novartis, Biogen, Roche, Lundberg, and Abbvie. He is a site co-investigator for Lilly/Avid and Janssen, and receives research support for clinical trials from Eisai, Lilly, and Cerveau. RAS has served as a paid consultant for Ionis, Shionogi, Biogen, Genentech, Oligomerix, Cytox, Acumen, JOMDD, Renew, Neuraly, AC Immune, Alnylam, Janssen, Neurocentria, Prothena, Eisai, Takeda and Roche and receives research support for clinical trials from Eisai, Eli Lilly, NIA and Alzheimer's Association. These relationships are not related to the content in the manuscript. All other authors report no relevant conflicts.

References

[1]. Braak H, Braak E. Neuropathological stageing of Alzheimer-related changes. Acta neuropathologica. 1991;82:239–59. [PubMed: 1759558]

[2]. Braak H, Thal DR, Ghebremedhin E, Del Tredici K. Stages of the pathologic process in Alzheimer disease: age categories from 1 to 100 years. J Neuropathol Exp Neurol. 2011;70:960–9. [PubMed: 22002422]

[3]. Nelson PT, Alafuzoff I, Bigio EH, Bouras C, Braak H, Cairns NJ, et al. Correlation of Alzheimer disease neuropathologic changes with cognitive status: a review of the literature. J Neuropathol Exp Neurol. 2012;71:362–81. [PubMed: 22487856]

[4]. Braak H, Del Tredici K. The pathological process underlying Alzheimer's disease in individuals under thirty. Acta neuropathologica. 2011;121:171–81. [PubMed: 21170538]

[5]. Ehrenberg AJ, Nguy AK, Theofilas P, Dunlop S, Suemoto CK, Di Lorenzo Alho AT, et al. Quantifying the accretion of hyperphosphorylated tau in the locus coeruleus and dorsal raphe nucleus: the pathological building blocks of early Alzheimer's disease. Neuropathol Appl Neurobiol. 2017;43:393–408. [PubMed: 28117917]

[6]. Sara SJ. The locus coeruleus and noradrenergic modulation of cognition. Nat Rev Neurosci. 2009;10:211–23. [PubMed: 19190638]

[7]. Jacobs HIL, Becker JA, Kwong K, Engels-Dominguez E, Prokopiou PC, Papp KV, et al. In vivo and neuropathology data support locus coeruleus integrity as indicator of Alzheimer's disease pathology and cognitive decline. Sci Transl Med. 2021;13:eabj2511. [PubMed: 34550726]

[8]. Betts MJ, Kirilina E, Otaduy MCG, Ivanov D, Acosta-Cabronero J, Callaghan MF, et al. Locus coeruleus imaging as a biomarker for noradrenergic dysfunction in neurodegenerative diseases. Brain. 2019;142:2558–71. [PubMed: 31327002]

[9]. Quiroz YT, Sperling RA, Norton DJ, Baena A, Arboleda-Velasquez JF, Cosio D, et al. Association Between Amyloid and Tau Accumulation in Young Adults With Autosomal Dominant Alzheimer Disease. JAMA neurology. 2018;75:548–56. [PubMed: 29435558]

[10]. Gordon BA, Blazey TM, Christensen J, Dincer A, Flores S, Keefe S, et al. Tau PET in autosomal dominant Alzheimer's disease: relationship with cognition, dementia and other biomarkers. Brain. 2019;142:1063–76. [PubMed: 30753379]

[11]. Sanchez JS, Hanseeuw BJ, Lopera F, Sperling RA, Baena A, Bocanegra Y, et al. Longitudinal amyloid and tau accumulation in autosomal dominant Alzheimer's disease: findings from the Colombia-Boston (COLBOS) biomarker study. Alzheimers Res Ther 2021;13:27. [PubMed: 33451357]

[12]. Theofilas P, Ehrenberg AJ, Dunlop S, Di Lorenzo Alho AT, Nguy A, Leite REP, et al. Locus coeruleus volume and cell population changes during Alzheimer's disease progression: A stereological study in human postmortem brains with potential implication for early-stage biomarker discovery. Alzheimers Dement. 2017;13:236–46. [PubMed: 27513978]

[13]. Francis PT, Palmer AM, Sims NR, Bowen DM, Davison AN, Esiri MM, et al. Neurochemical studies of early-onset Alzheimer's disease. Possible influence on treatment. The New England journal of medicine. 1985;313:7–11. [PubMed: 2582256]

[14]. Sheline YI, Miller K, Bardgett ME, Csernansky JG. Higher cerebrospinal fluid MHPG in subjects with dementia of the Alzheimer type. Relationship with cognitive dysfunction. Am J Geriatr Psychiatry. 1998;6:155–61. [PubMed: 9581211]

[15]. Jacobs HIL, Riphagen JM, Ramakers I, Verhey FRJ. Alzheimer's disease pathology: pathways between central norepinephrine activity, memory, and neuropsychiatric symptoms. Mol Psychiatry. 2021;26:897–906. [PubMed: 31138892]

[16]. Riphagen JM, van Egroo M, Jacobs HIL. Elevated Norepinephrine Metabolism Gauges Alzheimer's Disease-Related Pathology and Memory Decline. J Alzheimers Dis. 2021;80:521–6. [PubMed: 33554915]

[17]. Acosta-Baena N, Sepulveda-Falla D, Lopera-Gomez CM, Jaramillo-Elorza MC, Moreno S, Aguirre-Acevedo DC, et al. Pre-dementia clinical stages in presenilin 1 E280A familial early-onset Alzheimer's disease: a retrospective cohort study. Lancet Neurol. 2011;10:213–20. [PubMed: 21296022]

[18]. Aguirre-Acevedo DC, Lopera F, Henao E, Tirado V, Munoz C, Giraldo M, et al. Cognitive Decline in a Colombian Kindred With Autosomal Dominant Alzheimer Disease: A Retrospective Cohort Study. JAMA neurology. 2016;73:431–8. [PubMed: 26902171]

[19]. Dale AM, Fischl B, Sereno MI. Cortical surface-based analysis. I. Segmentation and surface reconstruction. NeuroImage. 1999;9:179–94. [PubMed: 9931268]

[20]. Klein A, Andersson J, Ardekani BA, Ashburner J, Avants B, Chiang MC, et al. Evaluation of 14 nonlinear deformation algorithms applied to human brain MRI registration. NeuroImage. 2009;46:786–802. [PubMed: 19195496]

[21]. Clewett DV, Huang R, Velasco R, Lee TH, Mather M. Locus Coeruleus Activity Strengthens Prioritized Memories Under Arousal. J Neurosci. 2018;38:1558–74. [PubMed: 29301874]

[22]. Clewett DV, Lee TH, Greening S, Ponzio A, Margalit E, Mather M. Neuromelanin marks the spot: identifying a locus coeruleus biomarker of cognitive reserve in healthy aging. Neurobiol Aging. 2016;37:117–26. [PubMed: 26521135]

[23]. Garcia-Lorenzo D, Longo-Dos Santos C, Ewenczyk C, Leu-Semenescu S, Gallea C, Quattrocchi G, et al. The coeruleus/subcoeruleus complex in rapid eye movement sleep behaviour disorders in Parkinson's disease. Brain. 2013;136:2120–9. [PubMed: 23801736]

[24]. Braak H, Del Tredici K. Neuroanatomy and pathology of sporadic Alzheimer's disease. Switzerland: Springer International Publishing; 2015.

[25]. Johnson KA, Schultz A, Betensky RA, Becker JA, Sepulcre J, Rentz D, et al. Tau positron emission tomographic imaging in aging and early Alzheimer disease. Ann Neurol. 2016;79:110–9. [PubMed: 26505746]

[26]. Jacobs HIL, Hedden T, Schultz AP, Sepulcre J, Perea RD, Amariglio RE, et al. Structural tract alterations predict downstream tau accumulation in amyloid-positive older individuals. Nat Neurosci. 2018;21:424–31. [PubMed: 29403032]

[27]. Mormino EC, Betensky RA, Hedden T, Schultz AP, Amariglio RE, Rentz DM, et al. Synergistic effect of beta-amyloid and neurodegeneration on cognitive decline in clinically normal individuals. JAMA neurology. 2014;71:1379–85. [PubMed: 25222039]

[28]. Greve DN, Svarer C, Fisher PM, Feng L, Hansen AE, Baare W, et al. Cortical surface-based analysis reduces bias and variance in kinetic modeling of brain PET data. NeuroImage. 2014;92:225–36. [PubMed: 24361666]

[29]. Bakdash JZ, Marusich LR. Repeated Measures Correlation. Front Psychol. 2017;8:456. [PubMed: 28439244]

[30]. Grinberg LT, Rueb U, Heinsen H. Brainstem: neglected locus in neurodegenerative diseases. Frontiers in neurology. 2011;2:42. [PubMed: 21808630]

[31]. Lemere CA, Lopera F, Kosik KS, Lendon CL, Ossa J, Saido TC, et al. The E280A presenilin 1 Alzheimer mutation produces increased A beta 42 deposition and severe cerebellar pathology. Nature medicine. 1996;2:1146–50.

[32]. Gordon BA, Blazey TM, Su Y, Hari-Raj A, Dincer A, Flores S, et al. Spatial patterns of neuroimaging biomarker change in individuals from families with autosomal dominant Alzheimer's disease: a longitudinal study. Lancet Neurol. 2018;17:241–50. [PubMed: 29397305]

[33]. Shibata E, Sasaki M, Tohyama K, Kanbara Y, Otsuka K, Ehara S, et al. Age-related changes in locus ceruleus on neuromelanin magnetic resonance imaging at 3 Tesla. Magn Reson Med Sci. 2006;5:197–200. [PubMed: 17332710]

[34]. Liu KY, Acosta-Cabronero J, Cardenas-Blanco A, Loane C, Berry AJ, Betts MJ, et al. In vivo visualization of age-related differences in the locus coeruleus. Neurobiol Aging. 2019;74:101–11. [PubMed: 30447418]

[35]. Gomez-Isla T, Growdon WB, McNamara MJ, Nochlin D, Bird TD, Arango JC, et al. The impact of different presenilin 1 andpresenilin 2 mutations on amyloid deposition, neurofibrillary changes and neuronal loss in the familial Alzheimer's disease brain: evidence for other phenotype-modifying factors. Brain. 1999;122 (Pt 9):1709–19. [PubMed: 10468510]

[36]. Chen CD, Holden TR, Gordon BA, Franklin EE, Li Y, Coble DW, et al. Ante- and postmortem tau in autosomal dominant and late-onset Alzheimer's disease. Ann Clin Transl Neurol. 2020;7:2475–80. [PubMed: 33150749]

[37]. Shepherd C, McCann H, Halliday GM. Variations in the neuropathology of familial Alzheimer's disease. Acta neuropathologica. 2009;118:37–52. [PubMed: 19306098]

[38]. Abercrombie ED, Jacobs BL. Single-unit response of noradrenergic neurons in the locus coeruleus of freely moving cats. I. Acutely presented stressful and nonstressful stimuli. J Neurosci. 1987;7:2837–43. [PubMed: 3625275]

[39]. Dahl MJ, Mather M, Duzel S, Bodammer NC, Lindenberger U, Kuhn S, et al. Rostral locus coeruleus integrity is associated with better memory performance in older adults. Nat Hum Behav. 2019;3:1203–14. [PubMed: 31501542]

[40]. Berron D, Vogel JW, Insel PS, Pereira JB, Xie L, Wisse LEM, et al. Early stages of tau pathology and its associations with functional connectivity, atrophy and memory. Brain. 2021;144:2771–83. [PubMed: 33725124]

[41]. Sanchez JS, Becker JA, Jacobs HIL, Hanseeuw BJ, Jiang S, Schultz AP, et al. The cortical origin and initial spread of medial temporal tauopathy in Alzheimer's disease assessed with positron emission tomography. Sci Transl Med. 2021;13(577): 10.1126/scitranslmed.abc0655.

[42]. He Z, Guo JL, McBride JD, Narasimhan S, Kim H, Changolkar L, et al. Amyloid-beta plaques enhance Alzheimer's brain tau-seeded pathologies by facilitating neuritic plaque tau aggregation. Nature medicine. 2018;24:29–38.

[43]. Bateman RJ, Xiong C, Benzinger TL, Fagan AM, Goate A, Fox NC, et al. Clinical and biomarker changes in dominantly inherited Alzheimer's disease. The New England journal of medicine. 2012;367:795–804. [PubMed: 22784036]

[44]. Fagan AM, Xiong C, Jasielec MS, Bateman RJ, Goate AM, Benzinger TL, et al. Longitudinal change in CSF biomarkers in autosomal-dominant Alzheimer's disease. Sci Transl Med. 2014;6:226ra30.

[45]. Zhang F, Gannon M, Chen Y, Yan S, Zhang S, Feng W, et al. beta-amyloid redirects norepinephrine signaling to activate the pathogenic GSK3beta/tau cascade. Sci Transl Med. 2020;12(526): 10.1126/scitranslmed.aay6931.

[46]. Kang SS, Liu X, Ahn EH, Xiang J, Manfredsson FP, Yang X, et al. Norepinephrine metabolite DOPEGAL activates AEP and pathological Tau aggregation in locus coeruleus. J Clin Invest. 2020;130:422–37. [PubMed: 31793911]

[47]. MCDade EM, Bateman RJ. Tau PET in autosomal dominant Alzheimer disease: small window, big picture. JAMA neurology. 2019;75:536–8.

[48]. Jack CR Jr., Bennett DA, Blennow K, Carrillo MC, Dunn B, Haeberlein SB, et al. NIA-AA Research Framework: Toward a biological definition of Alzheimer's disease. Alzheimers Dement. 2018;14:535–62. [PubMed: 29653606]

[49]. Kelly SC, He B, Perez SE, Ginsberg SD, Mufson EJ, Counts SE. Locus coeruleus cellular and molecular pathology during the progression of Alzheimer's disease. Acta Neuropathol Commun. 2017;5:8. [PubMed: 28109312]

[50]. O'Dell TJ, Connor SA, Guglietta R, Nguyen PV. beta-Adrenergic receptor signaling and modulation of long-term potentiation in the mammalian hippocampus. Learn Mem. 2015;22:461–71. [PubMed: 26286656]

Highlights

- Locus coeruleus (LC) integrity declines 12 years before clinical onset in ADAD
- LC integrity declines earlier and faster in ADAD as compared to sporadic AD
- Reductions in LC integrity predict expansion of cortical tau in PSEN1 carriers
- Lower LC integrity is associated with worse memory performance in PSEN1carriers
- Lower LC integrity is a promising early prognostic indicator in preclinical ADAD

Research in context

Systematic review:

We searched PubMed for literature on imaging of the locus coeruleus (LC), tau, memory and Alzheimer's disease (AD). Prior studies suggest that the LC is affected very early in the disease process and that structural integrity of the LC may be related to these early pathological processes.

Interpretation:

Dedicated imaging of the LC revealed changes 12 years before clinical onset. Reduction in LC integrity predicted increases in cortical tau over 24 months. These findings confirm that LC integrity may be a proxy of tau-related processes and support LC integrity as marker of disease progression in preclinical autosomal dominant AD (ADAD).

Future directions:

Findings highlight the promise of LC integrity as indicator of disease progression starting in the preclinical phase of ADAD. Further work is needed to clarify the directionality and mechanism of tau spreading, and its associations with downstream processes, such as neurodegeneration and cognitive decline.

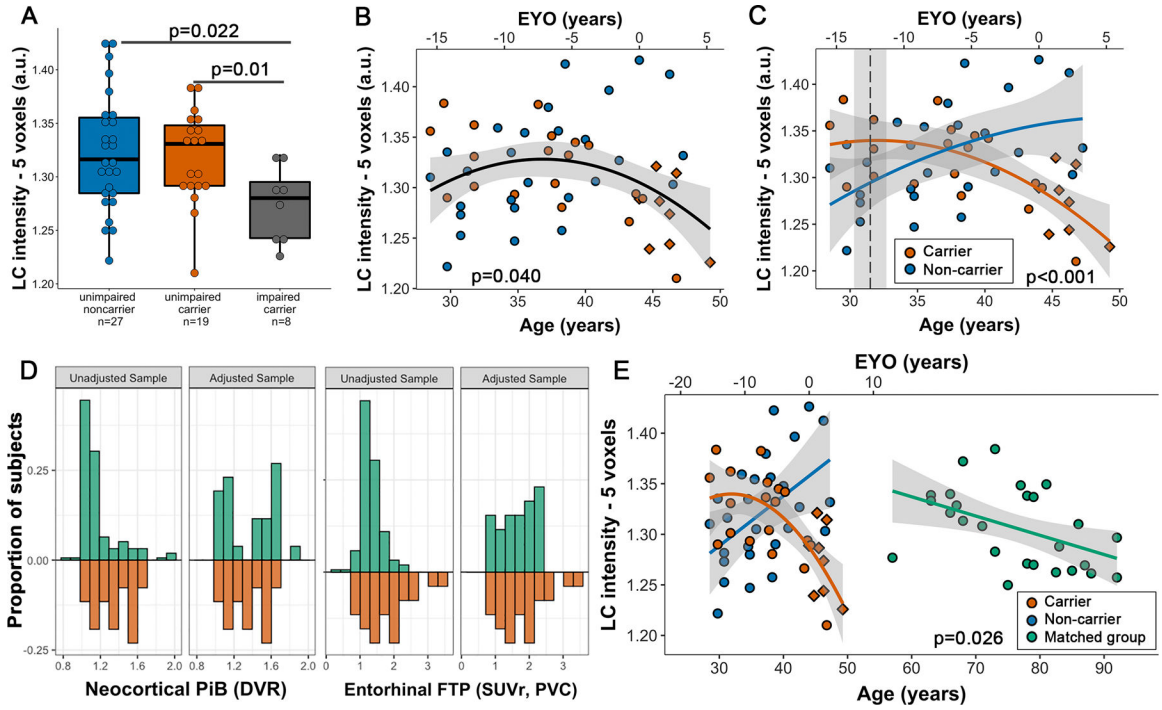

Figure 1: Relationship between LC intensity$_r$, group and age

Note: **A)** Boxplot showing group differences in LC intensity$_r$: impaired carriers had lower LC intensity$_r$ values compared to unimpaired carriers and noncarriers individuals. **B)** Across the entire group, we observed a nonlinear association with LC intensity$_r$ (n=54). **C)** Noncarriers show a positive age-relationship with LC intensity$_r$, while carriers show a negative age-relationship with the peak indicated by the dashed line (31.5 years). **D)** Distribution of PiB DVR and entorhinal FTP SUVr before (unadjusted) and after matching (adjusted) of the carriers (red) and the independent healthy sample (green). Proportion represents the relative frequency of subjects at a given level of biomarker burden. **E)** Comparison of the relationship between age and LC intensity$_r$ of carriers and a matched older group. Direction of the slope was similar, though the slope was steeper in the carriers. Shaded regions show the 95% confidence interval. Red diamond markers indicate the impaired carriers. Abbreviations: EYO = estimated years of onset

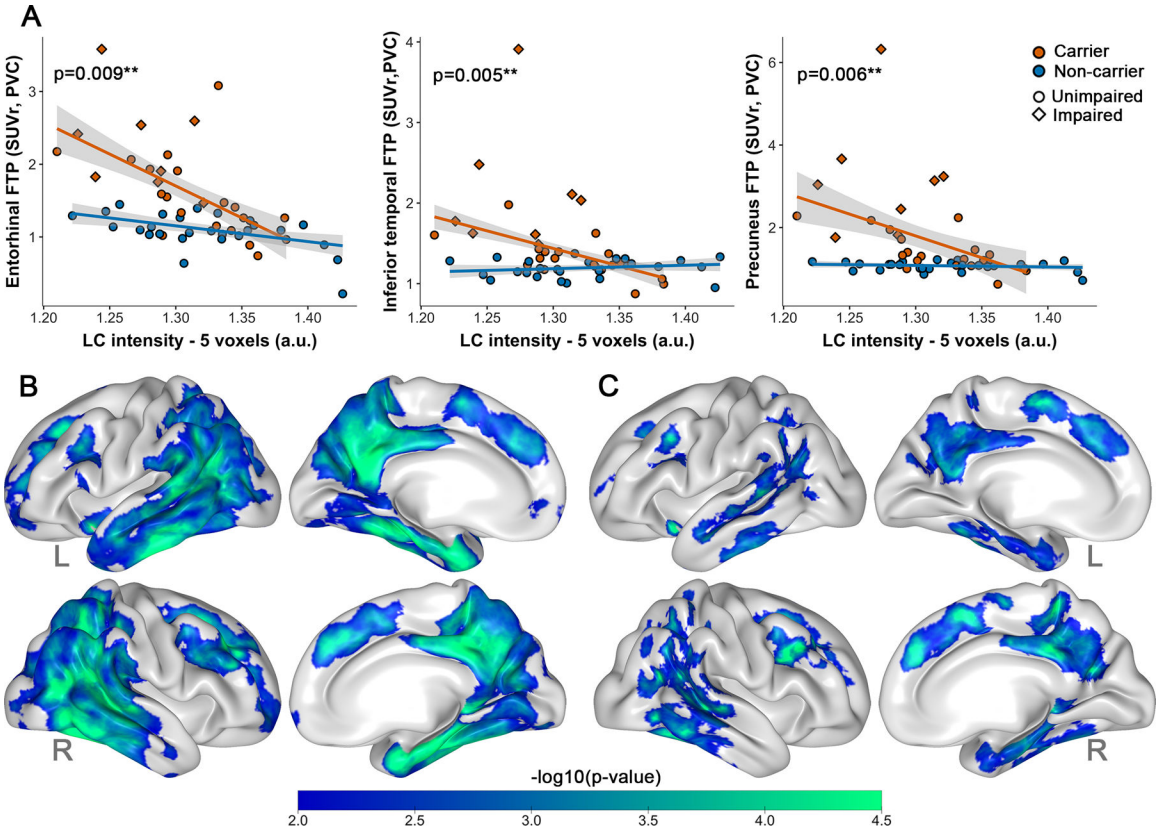

Figure 2: Associations between LC intensity$_r$ and tau binding

Note: **A)** ROI-based group differences (carriers n=27, noncarriers n=27) in the association between LC intensity$_r$ and FTP binding in the entorhinal cortex, inferior temporal cortex or the precuneus. PET-data was here partial volume corrected using the GTM-method. Shaded regions show the 95% confidence interval. **B)** Cortical vertex-wise FTP associations with LC intensity$_r$ in all carriers (n=27) **C)** Vertex-wise correlations with LC intensity$_r$ in the unimpaired carriers (n=19). Only negative associations were observed. The scale bar reflects the magnitude of the associations (green: greater effect size; blue: smaller effect size). Threshold was set at a cluster-corrected threshold of $p<0.01$ (expressed as -log10, min. cluster size of 120mm^2). PET surface data was adjusted for partial volume effects using the extended Müller-Gartner method. Abbreviations: L=left; R=right.

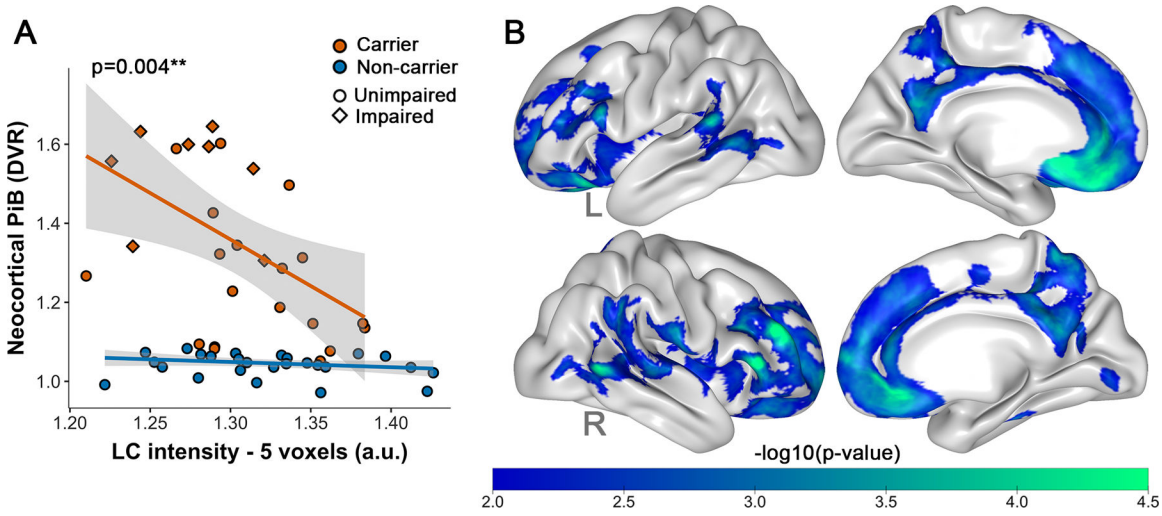

Figure 3: Associations between LC intensity$_r$ and Aβ deposition

Note: **A)** ROI-based group differences (carriers n=26, noncarriers n=27) in the association between LC intensity$_r$ and neocortical PiB binding. Shaded regions show the 95% confidence interval. **B)** Cortical vertex-wise PiB associations with LC intensity$_r$ in all carriers (n=26). Only negative associations were observed. The scale bar reflects the magnitude of the associations (green: greater effect size; blue: smaller effect size). Threshold was set at a cluster-corrected threshold of $p<0.01$ (expressed as -log10, min. cluster size of 120mm^2). Abbreviations: L=left; R=right

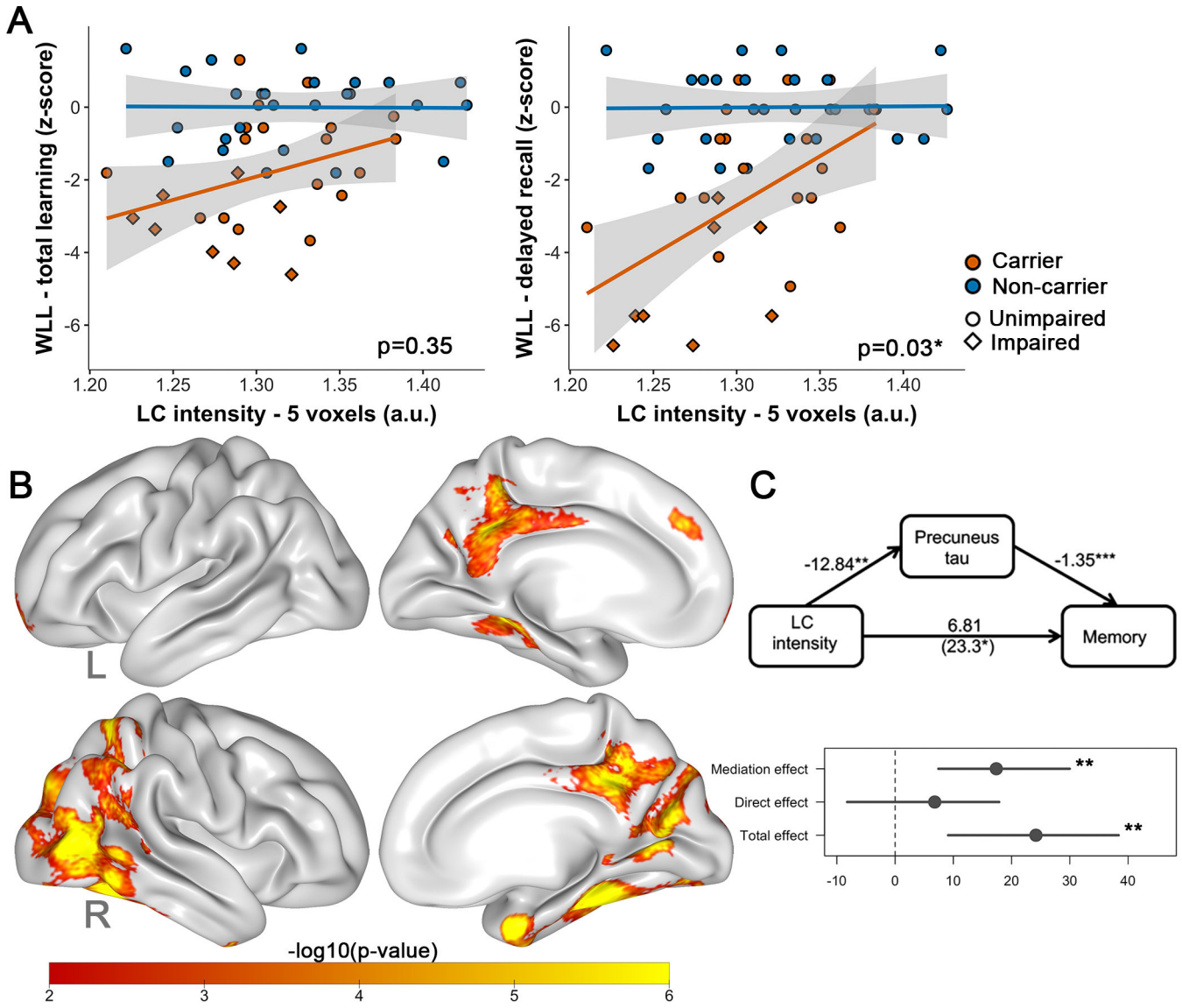

Figure 4: Associations between LC intensity$_r$ and memory performance

Note: **A)** Differences between carriers (n=26) and noncarriers (n=27) in the association between LC intensity$_r$ and memory (left: learning, right: delayed recall). Shaded regions show the 95% confidence interval. **B)** Quasi-Bayesian Monte Carlo Mediation results: vertex-wise analyses showing which tau regions (FTP SUVr, PVC) mediated the relationship between LC intensity$_r$ and memory in the carriers (n=26). Analyses were corrected for multiple comparisons using a cluster-wise correction at $p<0.01$. The scale bar reflects the magnitude of the probability of the indirect (mediation) effect (expressed in -log10(p-value); yellow: greater; red: smaller). **C)** ROI-based analyses (precuneus) confirming that precuneus FTP (SUVr, PVC) mediates the relationship between LC intensity$_r$ and memory. Abbreviations: WLL= word list learning, L=left, R=right

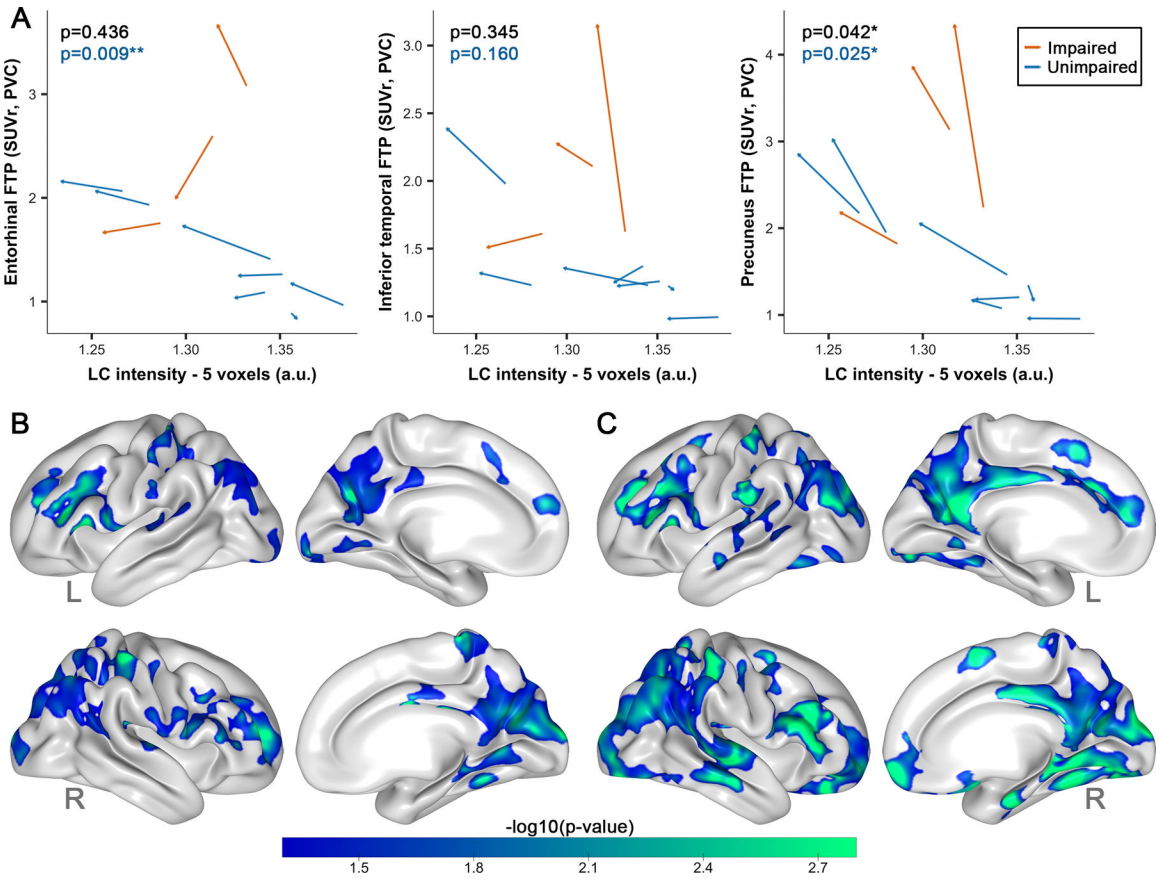

Figure 5: Associations between change in LC intensity$_r$ and change in tau pathology

Note: **A)** ROI-based associations between change in LC intensity$_r$ and FTP binding in the entorhinal cortex, inferior temporal cortex or the precuneus in the carriers (n=10). PET-data was partial volume corrected using the GTM-method. P-values in black refer to all carriers, in blue to the unimpaired carriers. **B)** Cortical vertex-wise FTP repeated measure correlations with LC intensity$_r$ over two time points in all carriers (n=10) and in the **C)** unimpaired carriers (n=7). The scale bar reflects the magnitude of the associations (green: greater effect size; blue: smaller effect size). Threshold was set at a cluster-corrected threshold of $p<0.05$ (expressed as -log10, min. cluster size of 120mm^2). PET surface data was adjusted for partial volume effects using the extended Müller-Gartner method. Abbreviations: L=left; R=right.

Table 1:

Demographics of the carriers and noncarriers

	Unimpaired Carriers (n=19)	Impaired Carriers (n=8)	Noncarriers (n=27)	p-value	
				All C vs NC	UnimpC vs NC
Age (years)	35.70 [31.75, 39.75]	45.88 [45.13, 46.38]	35.75 [32.38, 40.38]	0.10	0.88
(entire range)	[28.5, 46.75]	[44.0, 49.25]	[28.5, 47.25]		
Sex (n, % females)	10 (52.63%)	6 (75%)	17 (62.96%)	1	0.55
Education (years)	11 [5.0, 12.5]	6[^] [4.5, 12.0]	12.00 [10, 15]	0.06	0.12
MMSE score	28.0 [27.50, 29.0]	24.5 [21.75, 25.50]	29.0 [28.0, 30.0]	**<0.001**	0.05
FAST score	1.0 [1.0,1.5]	3.0 [3.0,3.0]	1.0 [10,1.0]	**0.004**	0.11
CERAD – word list total learning score	19 [14.50, 20.5]	11.5 [8.75, 13.25]	23 [19.50, 24.00]	**<0.001**	**0.003**
CERAD – word list delayed recall score	6.00 [5.00,8.00]	1.00 [0.75, 4.00]	8.00 [7.00, 9.00]	**<0.001**	**0.002**
Neocortical PiB (DVR)	1.25[^] [1.14, 1.34]	1.58 [1.49, 1.61]	1.05 [1.032, 1.065]	**<0.001**	**<0.001**
PiB positive (n, %)	11 (61%)	8 (100%)	0 (0%)	**<0.001**	**<0.001**
LC intensity$_r$	1.33 [1.29,1.34]	1.28 [1.24,1.30]	1.32 [1.28, 1.36]	0.31	0.98
	n=7	**Follow-up n=3**			
PET Follow-up time (years)	2.00 [2.00, 3.13]	1.75 [1.50, 2.88]			

Note: Group comparisons were performed with the Wilcoxon-signed rank test or the Fisher exact test. Demographics are expressed in median and interquartile interval for continuous variables and frequencies (n, %) for dichotomous variables.

[^]: 1 missing value.

Abbreviations: MMSE=Mini Mental State Examination, FAST=Functional Assessment Staging Tool, CERAD=Consortium to Establish a Registry for Alzheimer's Disease, PiB=Pittsburgh Compound B, DVR=Distribution volume ratio, LC=Locus Coeruleus, C=Carrier, NC=Noncarrier, UnimpC=Unimpaired Carrier.